Albumin Biomolecular Drug Designs Stabilized through Improved Thiol Conjugation and a Modular Locked Nucleic Acid Functionalized Assembly

Dinesen, Anders; Winther, Alexander; Wall, Archie; Märcher, Anders; Palmfeldt, Johan; Chudasama, Vijay; Wengel, Jesper; Gothelf, Kurt V.; Baker, James R.; Howard, Kenneth A.

Published in:
Bioconjugate Chemistry

DOI (link to publication from Publisher):
10.1021/acs.bioconjchem.1c00561

Publication date:
2022

Document Version
Publisher's PDF, also known as Version of record

Bioconjugate Chemistry

pubs.acs.org/bc

Article

Albumin Biomolecular Drug Designs Stabilized through Improved Thiol Conjugation and a Modular Locked Nucleic Acid Functionalized Assembly

Anders Dinesen, Alexander Winther, Archie Wall, Anders Märcher, Johan Palmfeldt, Vijay Chudasama, Jesper Wengel, Kurt V. Gothelf, James R. Baker, and Kenneth A. Howard*

Cite This: *Bioconjugate Chem.* 2022, 33, 333−342

Read Online

ACCESS | Metrics & More | Article Recommendations | Supporting Information

ABSTRACT: Albumin-nucleic acid biomolecular drug designs offer modular multifunctionalization and extended circulatory half-life. However, stability issues associated with conventional DNA nucleotides and maleimide bioconjugation chemistries limit the clinical potential. This work aims to improve the stability of this thiol conjugation and nucleic acid assembly by employing a fast-hydrolyzing monobromomaleimide (MBM) linker and nuclease-resistant nucleotide analogues, respectively. The biomolecular constructs were formed by site-selective conjugation of a 12-mer oligonucleotide to cysteine 34 (Cys34) of recombinant human albumin (rHA), followed by annealing of functionalized complementary strands bearing either a fluorophore or the cytotoxic drug monomethyl auristatin E (MMAE). Formation of conjugates and assemblies was confirmed by gel shift analysis and mass spectrometry, followed by investigation of serum stability, neonatal Fc receptor (FcRn)-mediated cellular recycling, and cancer cell killing. The MBM linker afforded rapid conjugation to rHA and remained stable during hydrolysis. The albumin-nucleic acid biomolecular assembly composed of stabilized oligonucleotides exhibited high serum stability and retained FcRn engagement mediating FcRn-mediated cellular recycling. The MMAE-containing assembly exhibited cytotoxicity in the human MIA PaCa-2 pancreatic cancer cell line with an IC50 of 342 nM, triggered by drug release from breakdown of an acid-labile linker. In summary, this work presents rHA-nucleic acid module-based assemblies with improved stability and retained module functionality that further promotes the drug delivery potential of this biomolecular platform.

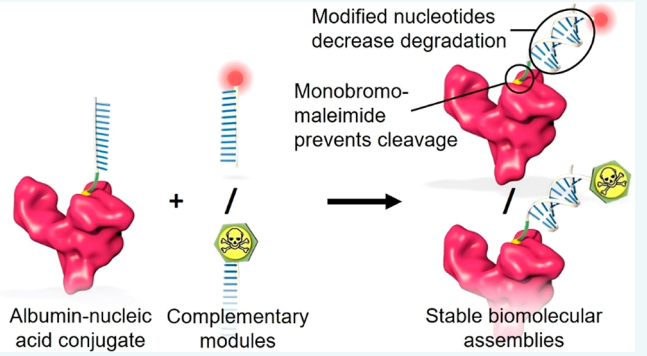

INTRODUCTION

Low molecular weight drugs and biomacromolecules are susceptible to rapid renal clearance and can, therefore, require half-life extension technologies to prolong their therapeutic effect.[1,2] Approaches to achieve this include the use of poly(ethylene glycol) (PEG)[3] or protein conjugation.[4] An attractive half-life extension approach is the utilization of albumin due to its extended circulatory half-life of approximately 19 days facilitated by engagement with the cellular recycling neonatal Fc receptor (FcRn).[5] Several albumin-binding drugs, albumin fusions, and albumin conjugates are on the market or are in clinical trials.[2,6,7] Site-selective conjugation of maleimide-functionalized drugs to albumin's single free thiol at cysteine 34 (Cys34) in albumin's domain I, distant from the main FcRn interaction interface at domain III, minimizes interference with the FcRn-mediated recycling process.[8] The reaction of maleimides' strong electrophilic carbon−carbon double bond with the nucleophilic thiolate on cysteine, forming a thiosuccinimide, is the fastest Michael addition reaction[9−12] and is widely used to conjugate drugs to proteins[13,14] including albumin[15] through bifunctional linkers or maleimide-functionalized drugs. The thiosuccinimide formed by the maleimide−thiol reaction, however, is susceptible to cleavage through a retro-Michael reaction reforming the starting maleimide that can undergo inactivating hydrolysis or thiol exchange in the presence of excess thiols.[16,17] Maleimide−albumin conjugates have been shown to exhibit premature payload release and exchange caused by this retro-Michael cleavage,[18,19] and similar observations have been made for antibody−drug conjugates.[20,21] Cleavage of the maleimide conjugates can be prevented by hydrolyzing the thiosuccinimide leading to a ring opening forming a stable succinamic acid thioether.[22,23] However, as shown by the Baker and Chudasama groups, hydrolysis can lead to loss of

Received: November 29, 2021
Revised: January 21, 2022
Published: February 7, 2022

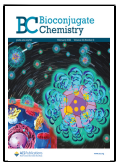

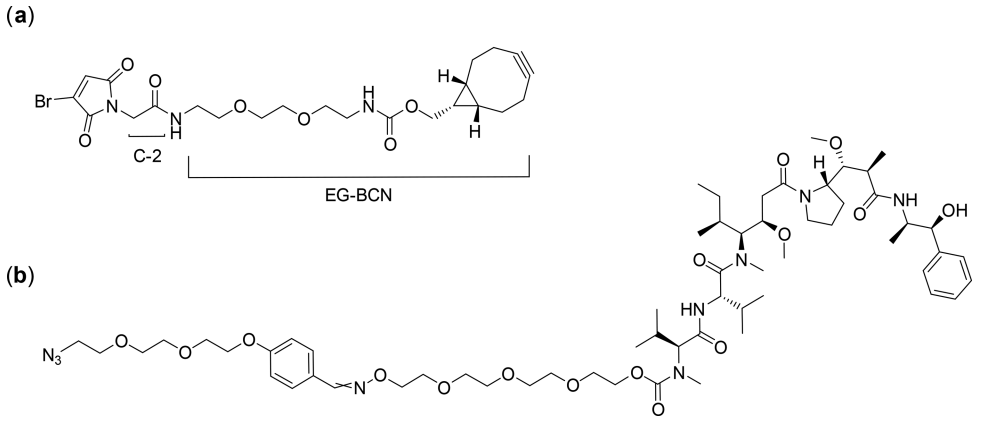

Figure 1. (a) Chemical structure of the monobromomaleimide (MBM)-bicyclo[6.1.0]nonyne (BCN) heterobifunctional linker. C-2: two-carbon spacer. EG-BCN: ethylene glycol-BCN. (b) Chemical structure of MMAE-azide.

Table 1. Oligonucleotides Used for Conjugation[a]

Oligo name	5′ modification	3′ modification	Sequence (5′-3′)
Q2(DNA)	NH_2-C_6	-	CAC AGT GGA CGG
cQ2(DNA)	NH_2-C_6	-	CCG TCC ACT GTG
Q2	NH_2-C_6	-	CAC AGT GGA CGG
cQ2	NH_2-C_6-TEG	-	CCG TCC ACT GTG
cQ2(PS)	NH_2-C_6-TEG	-	C*C*G* T*C*C* A*C*T* G*T*G
Q5-Cy5	NH_2-C_6	Cy5	CAA CCC ACA TAA AAG
cQ5	NH_2-C_6	-	C*T*T* T*T*A* T*G*T* G*G*G* T*T*G

[a]Black = DNA, blue = 2′-*O*-Me, red = LNA, * = PS bond, TEG = C_9 spacer.

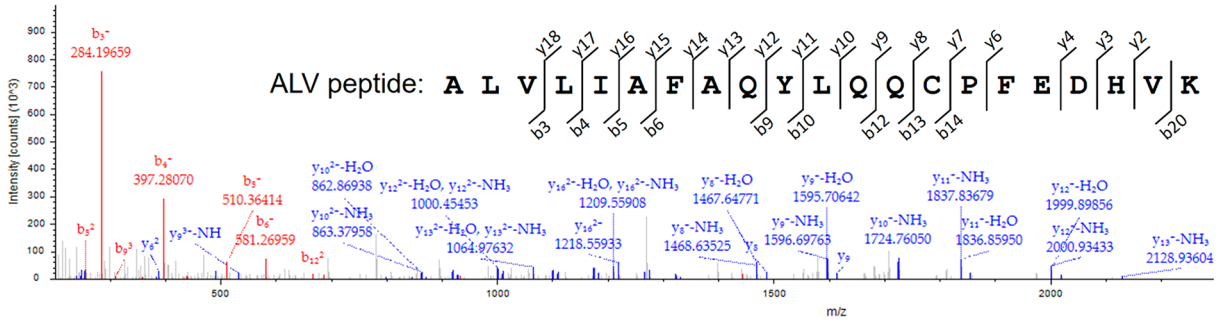

Figure 2. NanoLC-MS/MS data of the rHA−MBM-BCN linker conjugate. The Cys34-containing "ALV peptide" of rHA was detected with a mass matching the addition of the MBM-BCN linker (hydrolyzed and with an oxidation of the strained alkyne total monoisotopic peptide mass: 2944.5 Da). After peptide fragmentation, the fragments y8−y18, b14, and b20, containing the cysteine, carry the linker modification.

around half of the conjugate due to retro-Michael.[24] Therefore, several next-generation maleimides have been developed[25] including the monobromomaleimide (MBM) first developed by Baker and colleagues in 2009.[26] The bromine acts as a leaving group during conjugation to a thiol, preserving the maleimide unsaturation to form a thiomaleimide that prevents the retro-Michael reaction (Figure S1).[24] Further, the design of the MBM linker has been optimized to increase the rate of hydrolysis, facilitating production of stable thioether adducts in the conjugates.[27]

Single-site attachment at albumin's Cys34 limits drug payload capacity and inclusion of additional functional groups such as targeting moieties. Conjugation of nucleic acids to Cys34 allows generation of assemblies that act as scaffolds for incorporation of multiple drugs or functional groups into an albumin-nucleic acid biomolecular drug design.[28] Complementary strands bearing different functional groups offer a selective module-based approach for a specific application. We have previously introduced an albumin-nucleic acid biomolecular platform for functionalization with drugs or imaging agents using site-selective conjugation to Cys34 with standard maleimide chemistry.[28] However, this construct was comprised of DNA oligonucleotides susceptible to nuclease degradation, limiting its translational potential. The inclusion of locked

https://doi.org/10.1021/acs.bioconjchem.1c00561
Bioconjugate Chem. 2022, 33, 333−342

nucleic acid (LNA),[29,30] 2′-*O*-methyl (2′-*O*-Me),[31] and phosphorothioate (PS)[32] nucleotide modifications (Figure S2) preventing nuclease degradation offers a solution.

In this work, we address the stability issues of albumin-DNA biomolecular assemblies by utilizing an MBM linker (Figure 1(a)) for irreversible conjugation of nuclease-resistant LNA-, 2′-*O*-Me, and PS-modified oligonucleotides (Table 1). A novel MBM-bicyclo[6.1.0]nonyne (BCN) bifunctional linker was employed, as this allows for an efficient and versatile biomolecule conjugation with a tetrazine functionalized oligonucleotide. Biomolecular assemblies containing a fluorophore and the cytotoxic drug monomethyl auristatin E (MMAE) with an acid cleavable linker (Figure 1(b)) were successfully produced and exhibited stability, modular functionality, and FcRn-driven cellular recycling, furthering the translational potential of this biomolecular drug delivery platform.

RESULTS

Characterization of the rHA−MBM Linker Conjugate. The MBM-BCN linker (Figure 1a) was conjugated to rHA, and peptides obtained by trypsinization were investigated using nanoLC-MS/MS. The MS1 scan of the precursor peptide revealed a peptide with a mass corresponding to the Cys34-containing peptide ("ALV peptide", Figure 2) including the mass of the conjugated MBM-BCN linker (hydrolyzed to form the expected maleamic acid, and with the strained alkyne having undergone an oxidation and hydration (+34 Da addition),[33] during the digestion/nanoLC-MS/MS protocol; expected mass: 2944.48 Da, obtained mass: 2944.49 Da). Fragmentation of the ALV peptide confirmed peptide identity and revealed the modification site as being rHA's Cys34, as the mass of only the peptides containing the cysteine (y8−y18, b14, and b20) was increased with a mass corresponding to the MBM-BCN linker (Figure 2).

Absorbance at 350 nm was used to monitor thiomaleimide formed by conjugation of the MBM-BCN linker to rHA, yielding a $t_{99\%}$ of ∼17 min showing rapid conjugation (Figure 3(a)). Similarly, stabilizing hydrolysis of the thiomaleimide to maleamic acid was investigated by the decrease in 350 nm absorbance caused by the hydrolysis (Figure 3(b)). This indicated fast hydrolysis with a $t_{99\%}$ of ∼5 h under relatively mild conditions at pH 8.0 and 37 °C. Importantly, it was observed that hydrolysis does not lead to any detectable release of conjugated cargo, suggesting that no retro-Michael reaction occurs (Figure S3).

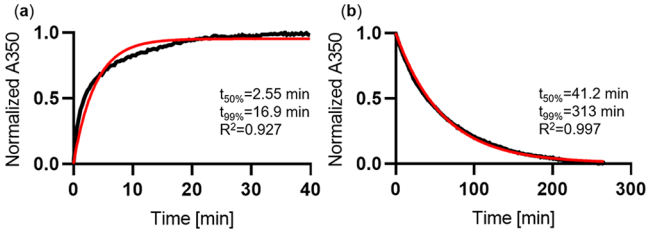

Figure 3. MBM-BCN and rHA reaction and hydrolysis kinetics. Black line: absorbance data, red line: data fit. (a) Increasing absorbance at 350 nm indicates formation of thiomaleimide by reaction of MBM-BCN with rHA. (b) Decreasing absorbance at 350 nm indicates hydrolysis of the rHA-conjugated thiomaleimide to maleamic acid.

Production of Albumin-Nucleic Acid Assemblies. The MBM-BCN linker conjugation to rHA was followed by attachment of an oligonucleotide termed Q2 previously modified with a tetrazine group (Figure S4). The complementary oligonucleotide (cQ2) was functionalized with Cy5.5 or MMAE and then annealed to form the biomolecular assembly.

Modification of the Q2 strand with a tetrazine moiety was shown by mobility shift on a SYBR Gold stained native PAGE gel (Figure 4(a)). The MBM-BCN linker was conjugated to albumin and, immediately after, conjugated to the tetrazine-modified Q2. HPLC IEX purification was performed to remove excess unconjugated reagents resulting in a pure rHA-Q2 sample (Figure 4(b) lane 3 and (f) peak 3).

cQ2 was functionalized with Cy5.5 or MMAE synthesized in-house with an acid cleavable linker (Figure 1(b)). The linker showed cleavage after incubation at pH 5.5 (Figure S9). Both the Cy5.5 and MMAE conjugates were purified by HPLC RP (Figure 4(g) and (h)) yielding functionalized cQ2 as confirmed by LC-MS (cQ2-Cy5.5 expected mass: 5129.4 Da, obtained mass: 5127.8 Da, cQ2-MMAE expected mass: 6065.6 Da, obtained mass: 6064.1 Da) with high purity confirmed by native PAGE (Figure 4(c) and (d)).

The rHA-Q2 and functionalized cQ2 were annealed with very high efficiency as confirmed by native PAGE yielding two different functionalized albumin-nucleic acid assemblies (Figure 4(e)).

To exemplify the multifunctionalization potential of the biomolecular assembly, annealing of two different fluorophore-bearing modules resulted in a dual fluorophore signal confirmed by native PAGE (Figure S10).

rHA-Q2/cQ2-Cy5.5 was produced employing different combinations of Q2(DNA), Q2 (i.e., with LNA and 2′-*O*-Me modifications), cQ2(DNA), cQ2 (LNA and 2′-*O*-Me modifications), and cQ2(PS) (PS modification in combination with LNA and 2′-*O*-Me), and stability was investigated in 50% FBS at 37 °C. Assembly stability was quantified by rHA-associated Cy5.5 fluorescence by native PAGE. This revealed that the Q2(DNA)/cQ2(DNA) homoduplex was almost completely degraded within 24 h, while incorporation of a single strand with stabilized nucleotides greatly improved serum stability (Figure 5). The greatest stability was achieved with Q2/cQ2(PS), where 85% of the annealed conjugate remained intact after 72 h. For this reason, the rHA-Q2/cQ2(PS) assembly was selected for subsequent cellular functional evaluation.

Cellular Functional Characterization of Albumin-Nucleic Acid Assemblies. FcRn-mediated cellular recycling was assessed for rHA and the rHA-nucleic acid assemblies (Figure 6). 55.1 pM rHA was recycled in the assay in accordance with previously published work,[5] while both rHA-nucleic acid assemblies underwent FcRn-mediated recycling to an even higher degree than rHA alone.

A cell-killing assay was performed in MIA PaCa-2 pancreatic cancer cells to investigate cytotoxic drug efficacy with the biomolecular assembly. While the rHA-Q2 control showed no cell killing over the investigated concentration range, toxicity of the MMAE-azide was observed with an IC50 of 79.9 nM (Figure 7). The stabilized biomolecular assembly employing LNA, 2′-*O*-Me, and PS oligonucleotides (rHA-Q2/cQ2(PS)-MMAE) exhibited lower toxicity with an IC50 of 342 nM. This is most likely due to steric effects from conjugation of the drug to the oligonucleotide and albumin in addition to the high

https://doi.org/10.1021/acs.bioconjchem.1c00561
Bioconjugate Chem. 2022, 33, 333−342

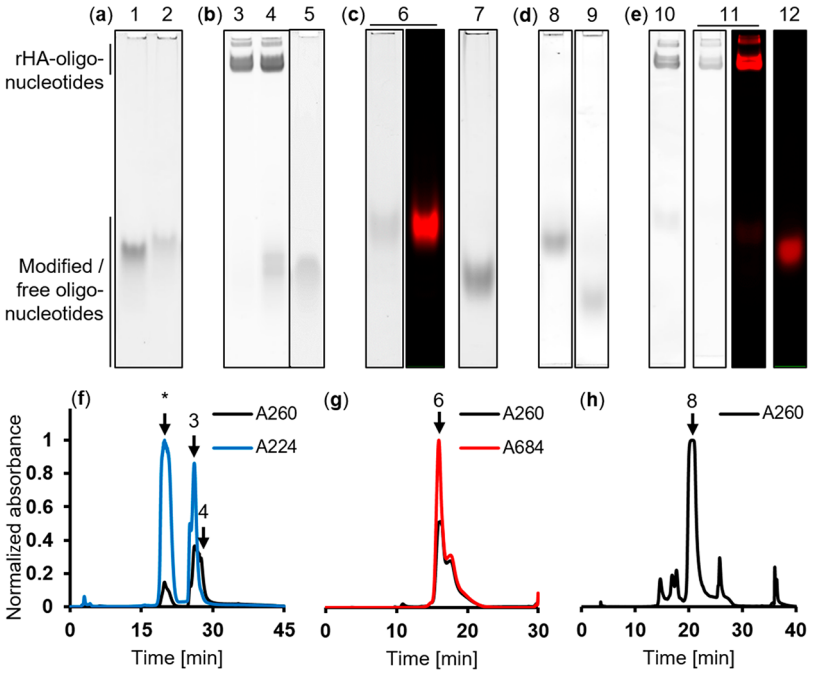

Figure 4. Conjugation and purification of rHA-nucleic acid assemblies. Black bands: SYBR gold signal, red bands: Cy5.5 fluorescence. A224, A260, and A684 indicate absorbance at 224, 260, and 684 nm, respectively. (a) Native PAGE of Q2-tetrazine. Lane 1: Q2, lane 2: Q2-tetrazine. (b) Native PAGE of HPLC purification of rHA-MBM-Q2. Lanes 3 and 4: HPLC IEX peaks 3 and 4 (as indicated in f), lane 5: Q2-tetrazine control. (c) Native PAGE of HPLC purification of cQ2(PS)-Cy5.5. Lane 6: HPLC RP peak 6 (as indicated in g), lane 7: cQ2(PS) control. (d) Native PAGE of HPLC purification of cQ2(PS)-MMAE. Lane 8: HPLC RP peak 8 (as indicated in h), lane 9: cQ2(PS) control. (e) Native PAGE of annealed albumin−nucleic acid conjugates. Lane 10: WT rHA-MBM-Q2/cQ2(PS)-MMAE, lane 11: WT rHA-MBM-Q2/cQ2(PS)-Cy5.5, lane 12: cQ2(PS)-Cy5.5 control. (f) HPLC IEX chromatogram showing purification of rHA-MBM-Q2. * indicates rHA peak. Peaks 3 and 4 were analyzed by native PAGE in subfigure (b) lanes 3 and 4. (g) HPLC RP chromatogram showing purification of cQ2(PS)-Cy5.5. Peak 6 was analyzed by native PAGE in subfigure (c). (h) HPLC RP chromatogram showing purification of cQ2(PS)-MMAE. Peak 8 was analyzed by native PAGE in subfigure (d). Data is representative of multiple repeated experiments.

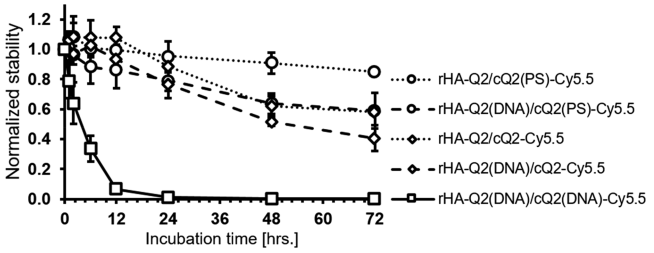

Figure 5. Serum stability of albumin-nucleic acid assemblies. Stability data is based on the Cy5.5 fluorescence signal of rHA-Q2/cQ2-Cy5.5 with different combinations of Q2(DNA), Q2, cQ2(DNA) cQ2, and cQ2(PS) normalized to 0 h. N = 2 independent experiments; error bars indicate SEM.

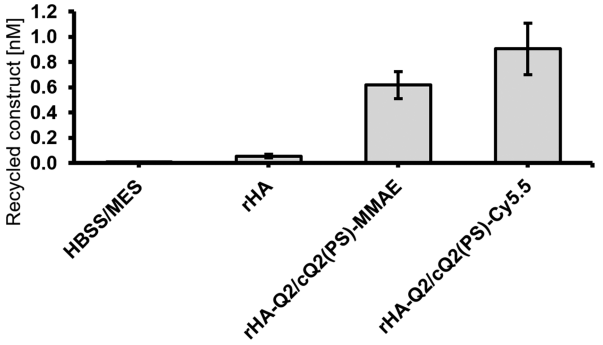

Figure 6. FcRn-mediated cellular recycling assay. ELISA detection of rHA and rHA−nucleic acid conjugates following FcRn-mediated cellular recycling in HMEC-1-FcRn expressing cells. HBSS/MES is a buffer control without any protein. N = 4 independent experiments; error bars indicate SEM.

stability of the LNA, which minimizes possible contribution by release of free MMAE through oligonucleotide degradation, and relies exclusively on drug release through cleavage of the acid-labile linker. In accordance with this, toxicity similar to that of MMAE-azide was observed for the unstabilized rHA-Q2(DNA)/cQ2(DNA)-MMAE construct probably due to the contribution by free drug release through oligonucleotide degradation (data not shown).

DISCUSSION

Albumin biomolecular assemblies that utilize nucleic acid scaffolds constitute modular systems to add functionality and maximize drug efficacy. These assemblies offer the potential to multifunctionalize with multiple cytotoxic drugs or include active targeting or imaging modalities for theranostic approaches.

This work aims to improve the translational potential of albumin-nucleic acid assemblies by increasing the stability of the maleimide−thiol conjugation and incorporated nucleic acids by employing an MBM linker and modified oligonucleotides, respectively.

The MBM-BCN linker was shown to rapidly conjugate to rHA, and in MS analysis, the mass of the Cys34-containing precursor peptide had an increased mass corresponding to the hydrolyzed MBM-BCN linker with an oxidized BCN group.

https://doi.org/10.1021/acs.bioconjchem.1c00561
Bioconjugate Chem. 2022, 33, 333−342

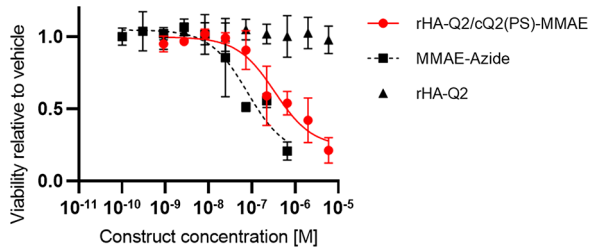

Figure 7. Cell-killing assay. Cell viability determined by the MTT assay in MIA PaCa-2 cells after incubation with rHA-Q2/cQ2(PS)-MMAE for 48 h and plotted relative to vehicle (annealing buffer). MMAE-azide: $N = 2$ and the remaining samples; $N = 3$ independent experiments; error bars indicate SEM.

Peptide fragmentation allowed determination of the exact conjugation site as being Cys34. After conjugation of the MBM-BCN linker alone to rHA, stabilizing hydrolysis proceeded under mild conditions (pH 8.0 at 37 °C for 5 h) without any release of conjugated cargo through the retro-Michael reaction. Hydrolysis is required after conjugation to prevent thiol exchange and consequent cargo transfer to other thiol-containing species present in blood (e.g., native serum albumin, cysteines, homocysteine, and glutathione).[20] However, Cys34 of albumin lies in an ∼10 Å deep hydrophobic crevice[6] discommoding hydrolysis.[20] The design of the MBM-BCN linker has, therefore, been optimized to facilitate the hydrolysis in this region by inclusion of an electron withdrawing C-2 spacer allowing hydrolysis within a few hours under mild conditions (pH 8.0 at 37 °C).[27] This is in contrast to the harsher conditions (pH > 9 at 37 °C overnight) needed for hydrolysis of standard maleimide[27] that can be problematic for payloads such as proteins, peptides, or small molecules susceptible to aggregation at high pH[34,35] and can also lead to loss of drug payload during the hydrolysis step.[24] Thus, the rapid reaction speed in combination with hydrolysis under mild conditions with no loss of payload makes MBM-based linkers ideal for production of various biomolecular assemblies.

The free BCN handle of the MBM-BCN linker after conjugation to albumin was utilized for conjugation of a stabilized oligonucleotide. Functionalized complementary oligonucleotides could be efficiently annealed, forming functional albumin-nucleic acid assemblies.

The stability of the albumin-nucleic acid assemblies was investigated in 50% serum, where increased stability was shown by employing combinations of LNA-, 2′-*O*-Me-, and PS-modified oligonucleotides compared to DNA.

Rapid degradation of unmodified nucleic acids by nucleases has been a major factor limiting *in vivo* use of nucleic acids.[36] This has led to a wide range of nucleotide modifications that have been used in this work, which all prevent degradation through endo- and exonuclease recognition, while the 2′-*O*-Me and LNA modifications also increase the duplex melting temperature.

Duplex denaturation and nuclease digestion can both result in breakdown of the annealed conjugate. The theoretical melting temperature of the DNA homoduplex used in this work is 54 °C[37] affording stability at physiological temperature, thereby suggesting nuclease digestion to be the major mode of degradation.

FcRn-mediated recycling is the predominant driving force of albumin's extended circulation *in vivo*[38] and has been utilized to extend the circulatory half-life of albumin drug designs.[39,40] Albumin's Cys34 is located distant from the main FcRn interaction interface, so site-selective conjugation at this site should maintain FcRn engagement. To this end, this work showed retained FcRn-engagement for rHA assemblies functionalized with both Cy5.5 and MMAE in a cellular recycling assay in human endothelial HMEC-1-FcRn cells.

Interestingly, increased cellular recycling was observed for both functionalized biomolecular assemblies, suggesting some additional mechanism to either increase the amount of endocytosis, exocytosis, or both. It is known that stabilizing oligonucleotide modifications can facilitate uptake of oligonucleotides,[41] and this could in turn lead to increased FcRn-mediated recycling.

We have previously shown that FcRn-driven cellular recycling observed in the *in vitro* recycling assay is a good predictor of an extended circulatory half-life of albumin-based designs[39,40] that supports the *in vivo* potential of the bimolecular assembly. Future *in vivo* work, however, is required to confirm that the observed FcRn-mediated cellular recycling of the biomolecular platform demonstrated in this work correlates with an extended circulation. To fully exemplify this for recombinant human albumin designs, the more physiologically relevant human FcRn/human albumin double transgenic mouse introduced by us[42] should be used to overcome the challenge of competition from endogenous mouse albumin in standard mouse models.

MMAE has been explored as a cytotoxic agent against cancer but, due to its extreme potency and low solubility, requires modification for successful delivery.[43] Association of MMAE to albumin could, therefore, potentially improve its therapeutic performance.

The cytotoxicity of the rHA-nucleic acid assembly functionalized with MMAE was shown with an IC50 of 342 nM. Conjugation of MMAE to cQ2 and annealing of cQ2-MMAE to rHA should both improve the drug's solubility and lower the toxicity compared to MMAE-azide alone, likely by decreased membrane permeability and steric hindrance effects. Importantly, our laboratory has recently shown that FcRn is overexpressed in cancerous tissue in several cancer types and that FcRn engagement leads to increased albumin accumulation at the tumor site,[44] meaning attachment to albumin may potentially mediate targeting of the MMAE construct to cancer tissue. Inclusion of an acid-sensitive linker in the design may allow MMAE release at the low endosomal pH during cellular recycling[45] or low pH environment found in cancer tissue.[46]

The drug to albumin ratio (DAR) could be increased to maximize potency by conjugation to surface lysine residues,[47,48] but this can lead to heterogeneous drug loading and potential interference with the FcRn binding interface. Our approach offers potential for increased DAR and incorporation of other functionalities such as imaging and targeting moieties, by site-selectively conjugation and module annealing at albumin's Cys34 distant from the main FcRn binding interface. Furthermore, utilization of a recently developed triple thiol rHA[49] or inclusion of more elaborate nucleic acid scaffolds potentiallyoffers multiple handles for conjugation.

In this work, an albumin−nucleic acid modular-based conjugate exhibited stability, FcRn-driven cellular recycling, and cancer cell toxicity that promotes its use for future *in vivo* applications.

https://doi.org/10.1021/acs.bioconjchem.1c00561
Bioconjugate Chem. 2022, 33, 333−342

MATERIALS AND METHODS

Materials. Recombinant human albumin (rHA) expressed in *Saccharomyces cerevisiae* was obtained from Sigma-Aldrich (cat# A6608).

The oligonucleotides used in this work are listed in Table 1. Oligonucleotides were purchased from Integrated DNA Technologies (Leuven, Belgium) or synthesized by Jesper Wengel, University of Southern Denmark.

Synthesis of MBM-BCN Linker. The synthesis of MBM-BCN is described in the Supporting Information.

Synthesis of MMAE-Azide. The synthesis of MMAE-azide is described in the Supporting Information.

Cell Lines and Cell Culture. All cells were cultured at 37 °C, 5% CO_2. MIA PaCa-2 cells (ATCC, cat# CRL-1420) in Dulbecco's modified eagle medium (DMEM, Gibco, cat# 41965-039) were supplemented with 10% fetal bovine serum (FBS, Gibco, cat# 10500-064) and 1% penicillin/streptomycin (P/S, Gibco, cat# 14140-122). FcRn-transduced human microvascular endothelial cell line-1 (HMEC-1-FcRn) cells were previously generated[5] and cultured in MCDB 131 medium (Life Technologies, cat# 10372-019) with 10 ng/mL human epidermal growth factor (Peprotech, cat# AF-100-15), 1 μg/mL hydrocortisone (Sigma, cat# H0888), 50 μg/mL Geneticin (Gibco, cat# 10131-035), 0.25 μg/mL Puromycin (Life Technologies, cat# A11138-03), 2 mM L-glutamine (Lonza, cat# BE17-605E), and 10% FBS. The cells were used between passage numbers 20 and 30.

NanoLC-MS/MS Analysis of the rHA−MBM-BCN Conjugate. rHA was conjugated to the MBM-BCN linker alone (see MBM-BCN Conjugation to rHA and Attachment of Oligonucleotide), and then trypsin wasdigested as follows: cold acetone was added in 6-fold volume excess to the rHA−MBM-BCN conjugate and incubated overnight. After centrifugation, the rHA pellet was aspirated, dried, resuspended in 100 μL of 100 mM triethylammonium bicarbonate (TEAB) and 5 μL of 200 mM tris(2-carboxyethyl)phosphine (TCEP), and incubated at 55 °C for 1 h to reduce cysteine residues. 5 μL of 375 mM iodoacetamide in TEAB was added and incubated for 30 min at room temperature (RT) to block cysteines. 2.5 μg of trypsin was then added per 100 μg of the rHA−MBM-BCN conjugate for digestion overnight at 37 °C with 400 rpm orbital shaking.

The peptides were purified with a C18 centrifugation column before nanoliquid chromatography-tandem mass spectrometry (nanoLC-MS/MS) analysis using an EASY nanoLC-1000 (Thermo Scientific) coupled to a Q Exactive HF-X Hybrid Quadrupole-Orbitrap Mass Spectrometer (Thermo Fisher Scientific). The peptides were trapped on a precolumn (PepMap 100, 2 cm, 75 μm i.d., 3 μm C18 particles, 100 Å, Thermo Scientific) followed by reverse-phase separation on a C18 column with an integrated emitter (EASY-Spray column, PepMap 25 cm, 75 μm i.d., 2 μm, 100 Å, Thermo Scientific). The peptides were separated in a 45 min linear gradient, from 4 to 40% acetonitrile in 0.1% formic acid at a flow rate of 300 nL/min. The MS was operated in a positive, data-dependent mode, automatically switching between precursor scanning (MS1) and fragmentation (MS2) acquisition. Resolution of MS1 was set to 60,000, and resolution of MS2 was set to 15,000. Up to ten of the most intense ions were fragmented (MS2) per every MS1 scan, by higher-energy C-trap dissociation (HCD).

Data from nanoLC-MS/MS were searched against an in-house created database containing the human proteome (20,151 human proteins from Uniprot) including rHA. Identification based on peptide mass and peptide fragmentation pattern was performed in Proteome Discoverer 2.3 (Thermo Fisher Scientific) using the Sequest algorithm. In the search, the possibility for 511.22 Da modification on cysteine (corresponding to the mass of the conjugated and hydrolyzed MBM-BCN linker with oxidized BCN) was included.

UV−Vis Measurements of the rHA−MBM-BCN Conjugate Reaction and Hydrolysis Kinetics. An Evolution 260 Bio UV−visible spectrophotometer (Thermo Scientific) was used for absorbance measurement in quartz cuvettes with a 1 cm path length. Samples were baseline corrected.

MBM-BCN linker (100 nmol, 5.0 equiv) in 10 μL of dimethyl sulfoxide (DMSO, Sigma, cat# 276855) was conjugated to rHA (20 nmol, 1.0 equiv) and diluted to 200 μL with 0.1 M 4-(2-hydroxyethyl)-1-piperazineethanesulfonic acid (HEPES, Sigma, cat# H4034) pH 7.0, incubating at 20 °C. The absorbance measurement at 350 nm indicates thiomaleimide formation.[27]

Hydrolysis was performed by adding 0.1 M HEPES pH 8.0 in a 9-fold volume excess and incubating at 37 °C. Decreasing absorbance at 350 nm indicates ring-opening of the thiomaleimide by hydrolysis.[27]

Data analysis was performed in GraphPad Prism (version 9.2.0) using a one-phase association model with Y_0 constrained to 0 or 1 for the normalized 350 nm absorbance measurement of the reaction or hydrolysis data, respectively.

MBM-BCN Conjugation to rHA and Attachment of Oligonucleotide. MBM-BCN linker (100 nmol, 5.0 equiv) in DMSO (10 μL) was conjugated to rHA (20 nmol, 1.0 equiv) and diluted to 200 μL with 0.1 M HEPES pH 7.0 by incubating for 15 min at RT with 650 rpm orbital shaking. Excess linker was removed by spin filtration through a 10 kDa molecular weight cutoff membrane filter (Merck, cat# UFC501096). The BCN-modified rHA (∼20 nmol, 1.0 equiv) in 0.1 M HEPES pH 7.0 (∼35 μL) was conjugated to 10 nmol (∼0.5 equiv) of tetrazine-modified Cy5.5 (Lumiprobe, cat# 170E0) in DMSO (1 μL) or tetrazine-modified oligonucleotide (see Oligonucleotide Functionalization) in nuclease-free water (NFW, Invitrogen, cat# AM9937) (20 μL) overnight at RT with 650 rpm orbital shaking.

The rHA−oligonucleotide conjugate was hydrolyzed by adding 0.1 M HEPES pH 8.0 in a 9-fold volume excess and incubating at 37 °C for at least 6 h with 650 rpm orbital shaking.

The rHA−oligonucleotide conjugate was purified with high-performance liquid chromatography (HPLC) using an ion-exchange (IEX) column (see Preparative IEX Chromatography) resulting in yields of >40% with respect to the starting amount of oligonucleotide.

Oligonucleotide Functionalization. *Q2-Tetrazine.* Tetrazine-$(PEG)_5$-NHS-ester linker (BroadPharm, cat# BP-22681, Figure S4) (500 nmol, 50 equiv) in DMSO (5 μL) was conjugated to Q2 oligonucleotide (10 nmol, 1.0 equiv) in NFW (10 μL) with 15 μL of DMSO and 30 μL of 0.1 M HEPES pH 8.0 incubating overnight at RT with 650 rpm orbital shaking. Excess linker was removed by ethanol precipitation (described below).

cQ2-Cy5.5. Cy5.5-NHS-ester linker (Lumiprobe, cat# 47020) (100 nmol, 20 equiv) in DMSO (10 μL) was conjugated to cQ2 oligonucleotide (5 nmol, 1.0 equiv) in

https://doi.org/10.1021/acs.bioconjchem.1c00561
Bioconjugate Chem. 2022, 33, 333−342

NFW (5 μL) with 10 μL of DMSO and 35 μL of 0.1 M HEPES pH 8.0 incubating overnight at RT with 650 rpm orbital shaking. Excess linker was removed by ethanol precipitation (described below), and the conjugate was purified with HPLC using a reversed-phase (RP) column (see Preparative RP Chromatography).

cQ2-MMAE. NHS-ester-dibenzocyclooctyne (DBCO) linker (Sigma, cat# 761524) (200 nmol, 20 equiv) in DMSO (2 μL) was conjugated to cQ2 oligonucleotide (10 nmol, 1.0 equiv) in NFW (10 μL) with 30 μL of DMSO and 70 μL of 0.1 M HEPES pH 8.0 incubating overnight at RT with 650 rpm orbital shaking. Excess linker was removed by ethanol precipitation (described below). The cQ2-DBCO in NFW (20 μL) was then conjugated to MMAE-azide (see Supporting Information) (20 nmol, ∼2 equiv) in DMSO (10 μL) by incubating overnight at RT with 650 rpm orbital shaking. Next, the conjugate was purified with HPLC using an RP column (see Preparative RP Chromatography).

Ethanol Precipitation of Oligonucleotide Conjugates. Oligonucleotide (1.25 vol. eq), absolute ethanol (EtOH, VWR, cat# 20821.310) (7.75 vol. eq), and 3 M sodium acetate (NaOAc, Sigma, cat# S2889) (1.00 vol. eq) were mixed and incubated at −18 °C for 2.5−3 h followed by centrifugation (17,000 g, 45 min). The pellet was aspirated, washed with EtOH, and centrifuged (17,000 g, 30 min). The pellet was dried for 10 min and dissolved in NFW or 0.1 M HEPES pH 7.0.

LC-MS Confirmation of Conjugation. LC-MS was used for confirmation of functionalized oligonucleotide masses as described in ref 50.

Preparative and Analytical HPLC. The HPLC system consists of a low pressure gradient (LPG)-3400RS pump, a variable wavelength detector (VWD)-3400RS, and an Ultimate 3000 automated fraction collector (AFC, all from Thermo Fisher Scientific). Samples were loaded using a 100 μL Hamilton syringe (Sigma-Aldrich) into a Rheodyne 9725i manual injector (Thermo Fisher Scientific) connected to a 500 μL polyether ether ketone (PEEK) sample loop. Samples were filtered with a 0.2 μm polypropylene (PP) filter (Kinesis, cat# ESF-PP-04-022) before injection on the HPLC.

Preparative IEX Chromatography. IEX chromatography was performed with a Mono Q 5/50 GL anion exchange column (Cytiva) with the following program at 0.3 mL/min: 5 min buffer A (20 mM Tris (Sigma, cat# T5941) and 10 mM NaCl (Acros Organics, cat# 207790010) at pH 7.6), a 25 min gradient to buffer B (20 mM Tris and 800 mM NaCl at pH 7.6), 5 min of buffer B, a 5 min gradient to buffer A, and finally 5 min of buffer A. Absorbance was measured at 224 and 260 nm. The collected fractions were desalted and concentrated by centrifugation through 10 or 30 kDa molecular weight cutoff membrane filters.

Preparative RP Chromatography. Preparative RP chromatography was performed with an XTerra MS C18 column (Waters) with the following program at 0.5 mL/min: 2.5−5 min buffer A (5% triethylammonium acetate (TEAA, Sigma, cat# 69372) and 5% acetonitrile (MeCN, VWR, cat# 83639.320) in Milli-Q water), a 17.5−20 min gradient to buffer B (100% MeCN), 5 min of buffer B, a 2.5−5 min gradient to buffer A, and last 2.5−5 min buffer A. Absorbance was measured at 260 and 684 nm. The solvent of the collected fractions was evaporated using a RVC 2-18 speed vacuum centrifuge (Martin Christ) and resuspended in NFW.

Analytical RP Chromatography. Analytical RP chromatography was performed with a PerfectSil 300 C4 column (MZ Analytical) running the following program at 0.7 mL/min: 5 min buffer A (0.1% trifluoroacetic acid (TFA, Sigma cat# T6508) in Milli-Q water), a 5 min gradient to 35% buffer B (75% isopropyl alcohol (VWR, cat# 20880.320) in Milli-Q water), a 25 min gradient to 60% buffer B, a 4 min gradient to 95% buffer B, 6 min of buffer B, a 5 min gradient to buffer A, and last 5 min buffer A. Absorbance was measured at 280 and 684 nm.

Annealing of Functionalized Oligonucleotides. For oligonucleotide annealing, complementary strands were added in equimolar amounts to a concentration of 200 mM potassium acetate (KOAc, Sigma, cat# P1190). The solution was heated to 55−60 °C and slowly cooled to RT over 1.5−2 h.

Oligonucleotide concentration was determined by absorbance at 260 nm, if necessary compensating for fluorophore absorbance (Cy5.5 260 nm correction factor (CF_{260}) is 0.07). rHA−nucleic acid conjugate concentration was determined using a bicinchoninic acid (BCA) assay (Thermo Scientific, cat# 23225) according to the manufacturer's protocol.

Gel Electrophoresis of Functionalized Oligonucleotides and Biomolecular Assemblies. Casting of 15% native PAGE gels: 5 mL of ProtoGel (National Diagnostics, cat# EC-890), 4 mL of Milli-Q water, 1 mL of 10X tris, borate, ethylenediamine tetraacetic acid (TBE, Thermo Fisher Scientific, cat# 15581-044), 100 μL of 10% ammonium persulfate (APS, Sigma, cat# A3678), and 10 μL of *N*,*N*,*N*′,*N*′-tetramethylethylenediamine (TEMED, Sigma, cat# T9281) were mixed and poured into 1 mm cassettes (Invitrogen, cat# NC2010), a 10- or 12-well comb (Invitrogen cat# NC3010 or NC3012) was inserted, and gels were polymerized for 45 min.

Native PAGE samples were mixed with loading buffer to 10% glycerol (VWR, cat# 24388.295) and 1 g/L Orange G (Sigma, cat# O3756) and loaded in a gel run using TBE running buffer. Gels were run at 125−150 V for 75−120 min at RT with an EPS 601 electrophoresis power supply (Amersham Biosciences).

SYBR Gold (Invitrogen, cat# S11494) staining was performed using 1X SYBR Gold in Milli-Q for 15 min. SYBR Gold and conjugated fluorophores were imaged on an Amersham Typhoon 5 (Cytiva).

Serum Stability Assay of Biomolecular Assemblies. rHA-Q2/cQ2-Cy5.5 conjugates were incubated in 50% FBS in PBS at 37 °C. Samples were stored at −18 °C after 0, 1, 2, 6, 12, 24, 48, and 72 h and subsequently analyzed by native PAGE using the Cy5.5 fluorescence signal to quantify the intact conjugate.

FcRn-Mediated Cellular Recycling Assay of Biomolecular Assemblies. The FcRn-mediated cellular recycling assay was performed according to Schmidt et al.[5] 100,000 HMEC-1-FcRn cells were seeded in a 48-well plate (Sarstedt, cat# 83.3923) coated with 100 μL of 1:30 GelTrex (Life Technologies, cat# A1413202) for 1 h at 37 °C and incubated until near confluent. HMEC-1-FcRn cells were washed twice with warm PBS before incubation with 300 μL of analyte (150.4 nM analyte in Hank's Balanced Salt Solution (Sigma, cat# H9269) adjusted to pH 6.0 with MES buffer (Sigma, cat# M1317)) for 1 h at RT. Cells were washed with 4 °C PBS, before incubation with 160 μL of serum-free medium for 1 h.

https://doi.org/10.1021/acs.bioconjchem.1c00561
Bioconjugate Chem. 2022, 33, 333−342

The supernatant was harvested, and the amount of recycled analyte was quantified by sandwich ELISA.

96-well plates were coated with antialbumin capture antibody (Sigma, cat# A7544) 1:1000 in PBS for 2 h at RT, blocked with 2% mPBS for 2 h at RT, and washed with 0.05% PBST before incubation overnight at 4 °C with recycling samples and standard of the corresponding analytes. Wells were washed, incubated for 2 h at RT with HRP-conjugated anti-albumin antibody (Abcam, cat# ab8941, diluted 1:5000 in 2% mPBS), and washed again, and TMB was added. The reaction was stopped with 0.2 M H_2SO_4, and the absorbance at 450 nm was measured using a Clariostar plate reader with background subtraction of the absorbance at 655 nm. The data was analyzed using GraphPad Prism 9.2.0.

Cell Killing Assay of MMAE-Functionalized Biomolecular Assembly. 7,500 MIA PaCa-2 cells were seeded in a 96-well plate (Sarstedt, cat # 83.3924) previously coated with 50 μL of 1:50 GelTrex for 1 h at 37 °C. After 24 h, wells were aspirated, and the cells were incubated with medium containing analyte for 48 h.

The 3-(4,5-dimethylthiazol-2-yl)-2,5-diphenyltetrazolium bromide (MTT) assay (Roche, cat# 11 465 007 001) was performed according to the manufacturer's protocol. Cells were incubated with the MTT reagent for 30−45 min, and absorbance was measured at 570 nm (data) and 690 nm (background) using a Clariostar plate reader. Data was analyzed using a four-parameter logistic curve in Graphpad Prism 9.2.0.

■ ASSOCIATED CONTENT

Supporting Information

The Supporting Information is available free of charge at https://pubs.acs.org/doi/10.1021/acs.bioconjchem.1c00561.

> Monobromomaleimide reaction with albumin, MBM-BCN linker hydrolysis stability, chemical structure of stabilized nucleic acid analogues and tetrazine-$(PEG)_5$-NHS-ester linker, description of synthesis of MBM-BCN and MMAE-azide linkers, and multifunctionalized albumin biomolecular assembly (PDF)

■ AUTHOR INFORMATION

Corresponding Author

Kenneth A. Howard − *Interdisciplinary Nanoscience Center (iNANO) and Department of Molecular Biology and Genetics, Aarhus University, DK-8000 Aarhus C, Denmark;* orcid.org/0000-0002-9407-278X; Email: kenh@inano.au.dk

Authors

Anders Dinesen − *Interdisciplinary Nanoscience Center (iNANO) and Department of Molecular Biology and Genetics, Aarhus University, DK-8000 Aarhus C, Denmark*

Alexander Winther − *Interdisciplinary Nanoscience Center (iNANO) and Department of Molecular Biology and Genetics, Aarhus University, DK-8000 Aarhus C, Denmark*

Archie Wall − *Department of Chemistry, University College London, London WC1H 0AJ, U.K.*

Anders Märcher − *Interdisciplinary Nanoscience Center (iNANO) and Department of Chemistry, Aarhus University, DK-8000 Aarhus C, Denmark*

Johan Palmfeldt − *Research Unit for Molecular Medicine, Department of Clinical Medicine, Aarhus University, DK-8200 Aarhus N, Denmark*

Vijay Chudasama − *Department of Chemistry, University College London, London WC1H 0AJ, U.K.;* orcid.org/0000-0002-8876-3285

Jesper Wengel − *Nucleic Acid Center, Department of Physics, Chemistry, and Pharmacy, University of Southern Denmark, DK-5230 Odense M, Denmark;* orcid.org/0000-0001-9835-1009

Kurt V. Gothelf − *Interdisciplinary Nanoscience Center (iNANO) and Department of Chemistry, Aarhus University, DK-8000 Aarhus C, Denmark;* orcid.org/0000-0003-2399-3757

James R. Baker − *Department of Chemistry, University College London, London WC1H 0AJ, U.K.;* orcid.org/0000-0002-7223-2279

Complete contact information is available at: https://pubs.acs.org/10.1021/acs.bioconjchem.1c00561

Notes

The authors declare no competing financial interest.

■ ACKNOWLEDGMENTS

This research was funded by the Novo Nordisk Foundation, Grant; CEMBID (Center for Multifunctional Biomolecular Drug Design, Grant Number: NNF17OC0028070) and the Villum Fonden, Grant; BioNEC (Biomolecular Nanoscale Engineering Center, Grant Number: VKR18333). The authors also gratefully acknowledge EPSRC and Albumedix for funding A.W. The authors would like to thank Marwa Gaber Mohamed M Elkhashab for design of fluorophore-bearing oligonucleotide modules.

■ ABBREVIATIONS

2′-*O*-Me, 2′-*O*-methyl; CF260, 260 nm correction factor; MTT, 3-(4,5-dimethylthiazol-2-yl)-2,5-diphenyltetrazolium bromide assay; HEPES, 4-(2-hydroxyethyl)-1-piperazineethanesulfonic acid; MeCN, acetonitrile; APS, ammonium persulfate; ADCs, antibody−drug conjugates; BCA, bicinchoninic acid; BCN, bicyclo[6.1.0]nonyne; Cys34, cysteine 34; CEMBID, Center for Multifunctional Biomolecular Drug Design; DBCO, dibenzocyclooctyne; DMSO, dimethyl sulfoxide; DAR, drug to albumin ratio; DMEM, Dulbecco's modified eagle medium; EtOH, ethanol; HMEC-1-FcRn, FcRn-transduced human microvascular endothelial cell line-1; HCD, higher-energy C-trap dissociation; HPLC, high-performance liquid chromatography; IEX, ion-exchange; LNA, locked nucleic acid; LPG, low pressure gradient; MBM, monobromomaleimide; MMAE, monomethyl auristatin E; TEMED, *N*,*N*,*N*′,*N*′-tetramethylethylenediamine; nanoLC-MS/MS, nanoliquid chromatography-tandem mass spectrometry; FcRn, neonatal Fc receptor; NFW, nuclease-free water; P/S, penicillin/streptomycin; PS, phosphorothioate; PEG, poly(ethylene glycol); PEEK, polyether ether ketone; PP, polypropylene; KOAc, potassium acetate; rHA, recombinant human albumin; RP, reversed-phase; RT, room temperature; NaOAc, sodium acetate; TEAB, triethylammonium bicarbonate; TEAA, triethylammonium acetate; TFA, trifluoroacetic acid; TCEP, tris(2-carboxyethyl)phosphine; TBE, tris, borate, ethylenediamine tetraacetic acid; VWD, variable wavelength detector

REFERENCES

(1) Markovsky, E.; Baabur-Cohen, H.; Eldar-Boock, A.; Omer, L.; Tiram, G.; Ferber, S.; Ofek, P.; Polyak, D.; Scomparin, A.; Satchi-Fainaro, R. Administration, distribution, metabolism and elimination of polymer therapeutics. *J. Controlled Release* **2012**, *161* (2), 446−60.

(2) Sleep, D.; Cameron, J.; Evans, L. R. Albumin as a versatile platform for drug half-life extension. *Biochim. Biophys. Acta* **2013**, *1830* (12), 5526−34.

(3) Abuchowski, A.; van Es, T.; Palczuk, N. C.; Davis, F. F. Alteration of immunological properties of bovine serum albumin by covalent attachment of polyethylene glycol. *J. Biol. Chem.* **1977**, *252* (11), 3578−81.

(4) Szlachcic, A.; Zakrzewska, M.; Otlewski, J. Longer action means better drug: tuning up protein therapeutics. *Biotechnol. Adv.* **2011**, *29* (4), 436−41.

(5) Schmidt, E. G. W.; Hvam, M. L.; Antunes, F.; Cameron, J.; Viuff, D.; Andersen, B.; Kristensen, N. N.; Howard, K. A. Direct demonstration of a neonatal Fc receptor (FcRn)-driven endosomal sorting pathway for cellular recycling of albumin. *J. Biol. Chem.* **2017**, *292* (32), 13312−13322.

(6) Pilati, D.; Howard, K. A. Albumin-based drug designs for pharmacokinetic modulation. *Expert Opin. Drug Metab. Toxicol.* **2020**, *16* (9), 783−795.

(7) Larsen, M. T.; Kuhlmann, M.; Hvam, M. L.; Howard, K. A. Albumin-based drug delivery: harnessing nature to cure disease. *Mol. Cell. Ther.* **2016**, *4*, 3.

(8) Petersen, S. S.; Kläning, E.; Ebbesen, M. F.; Andersen, B.; Cameron, J.; Sørensen, E. S.; Howard, K. A. Neonatal Fc Receptor Binding Tolerance toward the Covalent Conjugation of Payloads to Cysteine 34 of Human Albumin Variants. *Mol. Pharm.* **2016**, *13* (2), 677−82.

(9) Bednar, R. A. Reactivity and pH dependence of thiol conjugation to N-ethylmaleimide: detection of a conformational change in chalcone isomerase. *Biochemistry* **1990**, *29* (15), 3684−3690.

(10) Frayne, S. H.; Murthy, R. R.; Northrop, B. H. Investigation and Demonstration of Catalyst/Initiator-Driven Selectivity in Thiol-Michael Reactions. *J. Org. Chem.* **2017**, *82* (15), 7946−7956.

(11) Chan, J. W.; Hoyle, C. E.; Lowe, A. B.; Bowman, M. Nucleophile-Initiated Thiol-Michael Reactions: Effect of Organocatalyst, Thiol, and Ene. *Macromolecules* **2010**, *43* (15), 6381−6388.

(12) Nair, D. P.; Podgórski, M.; Chatani, S.; Gong, T.; Xi, W.; Fenoli, C. R.; Bowman, C. N. The Thiol-Michael Addition Click Reaction: A Powerful and Widely Used Tool in Materials Chemistry. *Chem. Mater.* **2014**, *26* (1), 724−744.

(13) Nejadmoghaddam, M. R.; Minai-Tehrani, A.; Ghahremanzadeh, R.; Mahmoudi, M.; Dinarvand, R.; Zarnani, A. H. Antibody-Drug Conjugates: Possibilities and Challenges. *Avicenna J. Med. Biotechnol.* **2019**, *11* (1), 3−23.

(14) Jain, N.; Smith, S. W.; Ghone, S.; Tomczuk, B. Current ADC Linker Chemistry. *Pharm. Res.* **2015**, *32* (11), 3526−40.

(15) Kratz, F. Albumin as a drug carrier: Design of prodrugs, drug conjugates and nanoparticles. *J. Controlled Release* **2008**, *132* (3), 171−183.

(16) Fontaine, S. D.; Reid, R.; Robinson, L.; Ashley, G. W.; Santi, D. V. Long-Term Stabilization of Maleimide−Thiol Conjugates. *Bioconjugate Chem.* **2015**, *26* (1), 145−152.

(17) Ponte, J. F.; Sun, X.; Yoder, N. C.; Fishkin, N.; Laleau, R.; Coccia, J.; Lanieri, L.; Bogalhas, M.; Wang, L.; Wilhelm, S.; et al. Understanding How the Stability of the Thiol-Maleimide Linkage Impacts the Pharmacokinetics of Lysine-Linked Antibody-Maytansinoid Conjugates. *Bioconjugate Chem.* **2016**, *27* (7), 1588−98.

(18) Baldwin, A. D.; Kiick, K. L. Tunable Degradation of Maleimide−Thiol Adducts in Reducing Environments. *Bioconjugate Chem.* **2011**, *22* (10), 1946−1953.

(19) Yang, B.; Kwon, I. Chemical Modification of Cysteine with 3-Arylpropriolonitrile Improves the In Vivo Stability of Albumin-Conjugated Urate Oxidase Therapeutic Protein. *Biomedicines* **2021**, *9* (10), 1334.

(20) Shen, B.-Q.; Xu, K.; Liu, L.; Raab, H.; Bhakta, S.; Kenrick, M.; Parsons-Reponte, K. L.; Tien, J.; Yu, S.-F.; Mai, E.; et al. Conjugation site modulates the in vivo stability and therapeutic activity of antibody-drug conjugates. *Nat. Biotechnol.* **2012**, *30* (2), 184−189.

(21) Jackson, D.; Atkinson, J.; Guevara, C. I.; Zhang, C.; Kery, V.; Moon, S. J.; Virata, C.; Yang, P.; Lowe, C.; Pinkstaff, J.; et al. In vitro and in vivo evaluation of cysteine and site specific conjugated herceptin antibody-drug conjugates. *PloS one* **2014**, *9* (1), No. e83865.

(22) Caspersen, M. B.; Kuhlmann, M.; Nicholls, K.; Saxton, M. J.; Andersen, B.; Bunting, K.; Cameron, J.; Howard, K. A. Albumin-based drug delivery using cysteine 34 chemical conjugates - important considerations and requirements. *Ther. Delivery* **2017**, *8* (7), 511−519.

(23) Alley, S. C.; Benjamin, D. R.; Jeffrey, S. C.; Okeley, N. M.; Meyer, D. L.; Sanderson, R. J.; Senter, P. D. Contribution of Linker Stability to the Activities of Anticancer Immunoconjugates. *Bioconjugate Chem.* **2008**, *19* (3), 759−765.

(24) Smith, M. E.; Caspersen, M. B.; Robinson, E.; Morais, M.; Maruani, A.; Nunes, J. P.; Nicholls, K.; Saxton, M. J.; Caddick, S.; Baker, J. R.; et al. A platform for efficient, thiol-stable conjugation to albumin's native single accessible cysteine. *Org. Biomol. Chem.* **2015**, *13* (29), 7946−9.

(25) Ravasco, J.; Faustino, H.; Trindade, A.; Gois, P. M. P. Bioconjugation with Maleimides: A Useful Tool for Chemical Biology. *Chem. Eur. J.* **2019**, *25* (1), 43−59.

(26) Tedaldi, L. M.; Smith, M. E.; Nathani, R. I.; Baker, J. R. Bromomaleimides: new reagents for the selective and reversible modification of cysteine. *Chem. Commun.* **2009**, No. 43, 6583−5.

(27) Wall, A.; Nicholls, K.; Caspersen, M. B.; Skrivergaard, S.; Howard, K. A.; Karu, K.; Chudasama, V.; Baker, J. R. Optimised approach to albumin−drug conjugates using monobromomaleimide-C-2 linkers. *Org. Biomol. Chem.* **2019**, *17* (34), 7870−7873.

(28) Kuhlmann, M.; Hamming, J. B. R.; Voldum, A.; Tsakiridou, G.; Larsen, M. T.; Schmøkel, J. S.; Sohn, E.; Bienk, K.; Schaffert, D.; Sørensen, E. S.; et al. An Albumin-Oligonucleotide Assembly for Potential Combinatorial Drug Delivery and Half-Life Extension Applications. *Mol. Ther. Nucleic Acids* **2017**, *9*, 284−293.

(29) Singh, S. K.; Koshkin, A. A.; Wengel, J.; Nielsen, P. LNA (locked nucleic acids): synthesis and high-affinity nucleic acid recognition. *Chem. Commun.* **1998**, No. 4, 455−456.

(30) Obika, S.; Nanbu, D.; Hari, Y.; Andoh, J.-i.; Morio, K.-i.; Doi, T.; Imanishi, T. Stability and structural features of the duplexes containing nucleoside analogues with a fixed N-type conformation, 2'-O,4'-C-methyleneribonucleosides. *Tetrahedron Lett.* **1998**, *39* (30), 5401−5404.

(31) Inoue, H.; Hayase, Y.; Imura, A.; Iwai, S.; Miura, K.; Ohtsuka, E. Synthesis and hybridization studies on two complementary nona(2′-*O*-Methyl)ribonucleotides. *Nucleic Acids Res.* **1987**, *15* (15), 6131−48.

(32) Vosberg, H. P.; Eckstein, F. Effect of deoxynucleoside phosphorothioates incorporated in DNA on cleavage by restriction enzymes. *J. Biol. Chem.* **1982**, *257* (11), 6595−9.

(33) Spangler, B.; Yang, S.; Baxter Rath, C. M.; Reck, F.; Feng, B. Y. A Unified Framework for the Incorporation of Bioorthogonal Compound Exposure Probes within Biological Compartments. *ACS Chem. Biol.* **2019**, *14* (4), 725−734.

(34) Chi, E. Y.; Krishnan, S.; Randolph, T. W.; Carpenter, J. F. Physical stability of proteins in aqueous solution: mechanism and driving forces in nonnative protein aggregation. *Pharm. Res.* **2003**, *20* (9), 1325−36.

(35) Tian, J.; Stella, V. J. Degradation of Paclitaxel and Related Compounds in Aqueous Solutions II: Nonepimerization Degradation Under Neutral to Basic pH Conditions. *J. Pharm. Sci.* **2008**, *97* (8), 3100−3108.

(36) Okholm, A. H.; Kjems, J. DNA nanovehicles and the biological barriers. *Adv. Drug Deliv. Rev.* **2016**, *106* (Pt A), 183−191.

(37) Owczarzy, R.; Tataurov, A. V.; Wu, Y.; Manthey, J. A.; McQuisten, K. A.; Almabrazi, H. G.; Pedersen, K. F.; Lin, Y.;

https://doi.org/10.1021/acs.bioconjchem.1c00561
Bioconjugate Chem. 2022, 33, 333−342

Garretson, J.; McEntaggart, N. O.; et al. IDT SciTools: a suite for analysis and design of nucleic acid oligomers. *Nucleic Acids Res.* **2008**, *36* (Web Server), W163−W169.
(38) Chaudhury, C.; Mehnaz, S.; Robinson, J. M.; Hayton, W. L.; Pearl, D. K.; Roopenian, D. C.; Anderson, C. L. The major histocompatibility complex-related Fc receptor for IgG (FcRn) binds albumin and prolongs its lifespan. *J. Exp Med.* **2003**, *197* (3), 315−322.
(39) Larsen, M. T.; Rawsthorne, H.; Schelde, K. K.; Dagnæs-Hansen, F.; Cameron, J.; Howard, K. A. Cellular recycling-driven in vivo half-life extension using recombinant albumin fusions tuned for neonatal Fc receptor (FcRn) engagement. *J. Controlled Release* **2018**, *287*, 132−141.
(40) Mandrup, O. A.; Ong, S. C.; Lykkemark, S.; Dinesen, A.; Rudnik-Jansen, I.; Dagnæs-Hansen, N. F.; Andersen, J. T.; Alvarez-Vallina, L.; Howard, K. A. Programmable half-life and anti-tumour effects of bispecific T-cell engager-albumin fusions with tuned FcRn affinity. *Commun. Biol.* **2021**, *4* (1), 310.
(41) Deprey, K.; Batistatou, N.; Kritzer, J. A. A critical analysis of methods used to investigate the cellular uptake and subcellular localization of RNA therapeutics. *Nucleic Acids Res.* **2020**, *48* (14), 7623−7639.
(42) Viuff, D.; Antunes, F.; Evans, L.; Cameron, J.; Dyrnesli, H.; Thue Ravn, B.; Stougaard, M.; Thiam, K.; Andersen, B.; Kjærulff, S.; et al. Generation of a double transgenic humanized neonatal Fc receptor (FcRn)/albumin mouse to study the pharmacokinetics of albumin-linked drugs. *J. Controlled Release* **2016**, *223*, 22−30.
(43) Newman, D. J.; Cragg, G. M. Current Status of Marine-Derived Compounds as Warheads in Anti-Tumor Drug Candidates. *Mar. Drugs* **2017**, *15* (4), 99.
(44) Larsen, M. T.; Mandrup, O. A.; Schelde, K. K.; Luo, Y.; Sørensen, K. D.; Dagnæs-Hansen, F.; Cameron, J.; Stougaard, M.; Steiniche, T.; Howard, K. A. FcRn overexpression in human cancer drives albumin recycling and cell growth; a mechanistic basis for exploitation in targeted albumin-drug designs. *J. Controlled Release* **2020**, *322*, 53−63.
(45) Rudnik-Jansen, I.; Howard, K. A. FcRn expression in cancer: Mechanistic basis and therapeutic opportunities. *J. Controlled Release* **2021**, *337*, 248−257.
(46) Tannock, I. F.; Rotin, D. Acid pH in tumors and its potential for therapeutic exploitation. *Cancer Res.* **1989**, *49* (16), 4373−84.
(47) Di Stefano, G.; Fiume, L.; Baglioni, M.; Bolondi, L.; Chieco, P.; Kratz, F.; Pariali, M.; Rubini, G. Efficacy of doxorubicin coupled to lactosaminated albumin on rat hepatocellular carcinomas evaluated by ultrasound imaging. *Dig. Liver Dis.* **2008**, *40* (4), 278−84.
(48) Burger, A. M.; Hartung, G.; Stehle, G.; Sinn, H.; Fiebig, H. H. Pre-clinical evaluation of a methotrexate-albumin conjugate (MTX-HSA) in human tumor xenografts in vivo. *Int. J. Cancer* **2001**, *92* (5), 718−24.
(49) Schelde, K. K.; Nicholls, K.; Dagnæs-Hansen, F.; Bunting, K.; Rawsthorne, H.; Andersen, B.; Finnis, C. J. A.; Williamson, M.; Cameron, J.; Howard, K. A. A new class of recombinant human albumin with multiple surface thiols exhibits stable conjugation and enhanced FcRn binding and blood circulation. *J. Biol. Chem.* **2019**, *294* (10), 3735−3743.
(50) Märcher, A.; Nijenhuis, M. A. D.; Gothelf, K. V. A Wireframe DNA Cube: Antibody Conjugate for Targeted Delivery of Multiple Copies of Monomethyl Auristatin E. *Angew. Chem. Int. Edit.* **2021**, *60*, 21691.

https://doi.org/10.1021/acs.bioconjchem.1c00561
Bioconjugate Chem. 2022, 33, 333−342